

Adiabatic contraction revisited: implications for primordial black holes

Fabio Capela,¹ Maxim Pshirkov,^{2,3,4} and Peter Tinyakov¹

¹*Service de Physique Théorique, Université Libre de Bruxelles (ULB),
CP225 Boulevard du Triomphe, B-1050 Bruxelles, Belgium*

²*Sternberg Astronomical Institute, Lomonosov Moscow State University,
Universitetsky prospekt 13, 119992, Moscow, Russia*

³*Pushchino Radio Astronomy Observatory, Astro Space Center,
Lebedev Physical Institute Russian Academy of Sciences, 142290 Pushchino, Russia*

⁴*Institute for Nuclear Research of the Russian Academy of Sciences, 117312, Moscow, Russia*

We simulate the adiabatic contraction of a dark matter (DM) distribution during the process of the star formation, paying particular attention to the phase space distribution of the DM particles after the contraction. Assuming the initial uniform density and Maxwellian distribution of DM velocities, we find that the number $n(r)$ of DM particles within the radius r scales like $n(r) \propto r^{1.5}$, leading to the DM density profile $\rho \propto r^{-1.5}$, in agreement with the Liouville theorem and previous numerical studies. At the same time, the number of DM particles $\nu(r)$ with periastra smaller than r is parametrically larger, $\nu(r) \propto r$, implying that many particles contributing at any given moment into the density $\rho(r)$ at small r have very elongated orbits and spent most of their time at distances larger than r . This has implications for the capture of DM by stars in the process of their formation. As a concrete example we consider the case of primordial black holes (PBH). We show that accounting for very eccentric orbits boosts the amount of captured PBH by a factor of up to 2×10^3 depending on the PBH mass, improving correspondingly the previously derived constraints on the PBH abundance.

PACS numbers:

I. INTRODUCTION

Astrophysical and cosmological observations have provided a compelling evidence that about 28% of the energy density of the Universe is contained in the form of a non-relativistic non-baryonic dark matter (DM) [1]. Despite the extensive experimental efforts, all the attempts at direct and indirect non-gravitational detection of this matter have been unsuccessful so far, so that the DM nature remains essentially unconstrained, leaving room for a diversity of candidates. It is often assumed that the DM is composed of some kind of new particles beyond the Standard Model — axion-like particles, sterile neutrinos, weakly interacting massive particles are the most common examples. However, other candidates such as primordial black holes (PBH) may provide a viable alternative. In the latter case, the bonus is that no new particles beyond the Standard Model are required.

Apart from direct and indirect searches, competitive constraints on DM properties may be obtained from observations of stars where the DM could have been accumulated and produced observable effects. In the Sun, the DM annihilation may result in the observable flux of high energy neutrinos [2]. DM may also induce abnormal asteroseismological effects [3] or suppress convection zones [4, 5] or even modify the transportation properties throughout the star [6, 7].

More catastrophic effects may result from the DM accumulation in compact stars such as neutrons stars (NSs) or white dwarfs (WDs). If the particles of DM are not self-annihilating (e.g., asymmetric dark matter), the accumulated amount of DM may become sufficient to form a black hole (BH) inside the compact star [8–10]. Because

of a much higher density of nuclear matter in compact stars as compared to main sequence stars, the accretion is sufficiently efficient to destroy the star in a short time (see Ref. [11] for a detailed discussion, including the role of the angular momentum). In this case mere observations of compact stars imply constraints on the DM properties [8–10].

The same considerations obviously apply to the DM composed of PBHs, in which case there is no need to accumulate DM in order to form a BH. If even a single PBH is captured by a compact star, the latter gets destroyed. Requiring that the probability of such an event is small leads to the constraints on the PBH abundance [12, 13].

The key quantity which determines the strength of the constraints is the amount of captured DM. There are two different capture mechanisms. A star can capture DM from its surrounding environment, such as the Galactic halo, during its lifetime. The DM particles passing through the star may interact with the nucleons, losing enough energy to become gravitationally bound [2, 14]. Then each subsequent orbit will also pass through the star, so that eventually, after many collisions, the DM particle will sink to the center of the star. Such capture process can accumulate a considerable amount of DM inside the compact star throughout its lifetime [8].

The DM could also be captured during the star formation. A main-sequence star is formed from the gravitational collapse of a prestellar core in a giant molecular cloud. In the course of this process, the DM that was initially gravitationally bound to the core undergoes adiabatic contraction, forming a cuspy profile centered at the star, with the density $\rho(r)$ behaving like $\rho(r) \propto r^{-3/2}$. Some of this DM ends up captured in-

side the star. This mechanism was first discussed in [13] where the constraints on the abundance of PBHs were derived. Note that the adiabatic contraction is a purely gravitational phenomenon that assumes nothing about the DM-to-nucleon cross section.

In this paper we study in more detail the adiabatic contraction of the DM distribution caused by the star formation process. Our purpose is to obtain a more precise estimate of the amount of the DM captured by a newly-formed star.

In Ref. [13], the amount of captured DM was estimated by taking the DM density profile after the contraction and integrating it over the volume of the newly-formed star. However, this is likely to be an underestimate, at least for some values of parameters. Indeed, in general, all particles that have orbits crossing the star will pass through the star again and again, and eventually will get captured if given enough time. The number of such particles is *larger* than the number of particles that are inside the star at any given moment, because the particles that spend only a fraction of time inside the star contribute to the amount of DM inside the star proportionally to this fraction, which is less than 1. Thus, the number of particles that could be captured (provided there is enough time) is larger than the number of DM particles inside the star.

To quantify this effect, we have performed a simulation of the adiabatic contraction process where we have measured, in addition to the density at a given distance, the number of particles that have orbits with the periastron smaller than given radius r . We have found that the number of such particles scales differently at small r than the number of particles that are within r at a given moment: while the latter behaves like $\propto r^{1.5}$ (which corresponds to the density having a spike $\rho \propto r^{-1.5}$), the former goes as r . This means that at small r there are much more particles that *ever pass* within r , than actually are within r at a given moment. If these particles have enough time to lose their energy and get captured, this would substantially boost the amount of captured DM and improve the constraints accordingly. For relevant values of parameters, the boost factor can be as large as $\sim 2 \times 10^3$.

When these considerations are applied to the case of PBH, the previously derived constraints get improved. The improvement factor depends on the PBH mass that determines the energy loss time, and can be as large as $\sim 2 \times 10^3$ depending on the efficiency of energy losses.

The rest of this paper is organized as follows. In Sect. II we discuss the capture of DM by adiabatic contraction during the star formation stage. In Sect. III we present the resulting constraints coming from the enhancement of the DM capture in the case the latter is composed of PBHs. Finally, in Sect. IV we present our conclusions.

II. ADIABATIC CONTRACTION OF DM DURING STAR FORMATION

In this section, we discuss the adiabatic contraction of DM during the process of star formation, paying particular attention to the final distribution of particle orbits.

A. Star formation and adiabatic contraction of DM

Stars are formed in giant molecular clouds (GMCs) with a typical mass of $10^5 - 10^6 M_\odot$ and density $\rho_B \sim 500 \text{ GeV/cm}^3$. Such GMCs are initially supported against gravitational collapse by several pressure components [15, 16]. When this support gets reduced due to dissipation, GMCs fragment into smaller clumps, each forming a protostar after the contraction of the gas. The newly formed protostars have a central blob and a surrounding disk of gas. Once the central part has accumulated most of its main-sequence mass from the surrounding disk of gas, it is considered to be a pre-main-sequence star. Note that such process takes much longer than the gravitational free-fall time $t_{\text{ff}} \sim (G\rho_0)^{-1/2}$, where ρ_0 is the average density of the protostar cloud. Note also that even at the initial stages the baryonic density is quite high, so for most environments the gravitational effect of the DM on the formation of stars is negligible. For all practical purposes, the behavior of DM is determined by the gravitational potential of the baryons.

The baryons contracting into a protostar create a time-dependent gravitational potential which drags the DM particles along with the contracting baryons. As a result, the DM distribution develops a density profile that is peaked in the core of the prestellar cloud. Since this process takes much more time than the free-fall time t_{ff} , certain quantities are adiabatically conserved, which may be used in analytic estimates, provided some simplifying assumptions are made about the particle orbits. In realistic cases, however, one has to resort to numerical simulations.

B. Simulation of DM orbits

The star formation stage relevant for this paper is the formation of the star from a pre-stellar core. We adopt the core parameters following Ref. [13], the typical values being the baryonic density $\rho \sim 5 \times 10^6 \text{ GeV/cm}^3$ and the size $\sim 5000 \text{ AU}$. This baryonic density is much larger than the DM density in any of the environments that will be considered in this paper, so we neglect the DM contribution to the gravitational potential. This simplifies the simulations enormously as the DM trajectories may be evolved, one at a time, in the same time-dependent gravitational potential created by the contracting baryons.

In the adiabatic approximation it is not important how exactly the gravitational potential changes — only the initial and final states matter. We have modeled the

gravitational potential of the contracting baryons by a two-component mass distribution: the uniform spherical cloud and a point mass in its center. The total mass of the cloud and the value of the central mass are chosen in such a way that the latter linearly grows from zero at $t = 0$ to the maximum value at $t = T$, while the former decreases from the maximum value to zero, the total mass of the system being constant. In order to satisfy the adiabatic condition, this change is performed slowly over a period of time T that is at least several times longer than the free fall time.

For the initial DM distribution we take a uniform distribution in space characterized by some background DM density $\bar{\rho}_{\text{DM}}$, and the Maxwellian distribution in velocities with the dispersion \bar{v} ,

$$dn = \bar{n}_{\text{DM}} \left(\frac{3}{2\pi\bar{v}^2} \right)^{3/2} \exp \left\{ \frac{-3v^2}{2\bar{v}^2} \right\} d^3v, \quad (1)$$

where $\bar{n}_{\text{DM}} = \rho_{\text{DM}}/m_{\text{DM}}$ is the mean DM number density. The assumption of the Maxwellian distribution in velocities is not an essential one, because only the particles that are gravitationally bound to the pre-stellar core are affected by the contraction of baryons. These particles have very small velocities as compared to \bar{v} even for \bar{v} as low as a few km/s. Thus, any distribution which is flat around $v \sim 0$ will produce the same results.

The simulation proceeds as follows. At $t = 0$ we inject a DM particle with a random uniformly distributed initial position and velocity (keeping in mind that at $v \ll \bar{v}$ the Maxwellian distribution reduces to a uniform one). If the particle is gravitationally bound at $t = 0$, it is evolved through the equations of motion, otherwise it is rejected. At a randomly chosen time $t > T$ (i.e., when the baryonic contraction is finished), we record the position r of the particle. We also calculate and record the periastron r_{min} and apastron r_{max} of the particle orbit (these, of course, do not depend on time once the contraction is finished). We have simulated about 3×10^7 trajectories in this way.

In order to resolve the density profile down to distances comparable to the radius of the newly-formed star $R_* \sim R_\odot$ one can use the fact that r_{max} and r_{min} completely determine the particle orbit. One may therefore boost the efficiency of the simulations by generating several values of r per orbit, provided that the sampling is done uniformly in time. In doing so, the actual simulation of the trajectory after the contraction is not needed: instead one can use the Kepler's second law, which states that an imaginary line connecting the particle's position to the center of the star sweeps out the same area in the same amount of time. Therefore, for the trajectory defined by the given values of r_{max} and r_{min} the quantity

$$\xi(x) = \frac{1}{2} - \frac{2}{\pi(1+\mathcal{R})} \sqrt{(\mathcal{R}-x)(x-1)} - \frac{1}{\pi} \arctan \left(\frac{1+\mathcal{R}-2x}{2\sqrt{(\mathcal{R}-x)(x-1)}} \right) \quad (2)$$

where $x = r/r_{\text{min}}$, $\mathcal{R} = r_{\text{max}}/r_{\text{min}}$ and $\xi = A/A_{\text{tot}}$ with

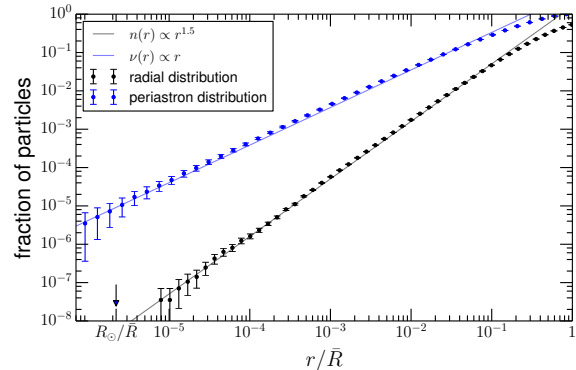


FIG. 1: *Lower curve:* The fraction of particles $n(r)$ that are found within radius r at the end of the adiabatic contraction. \bar{R} is the initial radius of the prestellar core. *Upper curve:* The fraction of particles $\nu(r)$ whose orbits have the periastron smaller than r . Lines show the power laws $n(r) \propto r^{1.5}$ and $\nu(r) \propto r$. The errorbars represent statistical errors.

A_{tot} half of the total area of the orbit, is proportional to the time. This function is constructed in such a way that $\xi(1) = 0$ and $\xi(\mathcal{R}) = 1$. Thus, one can generate a random uniformly distributed $\xi \in [0, 1]$ and solve eq. (2) for x , obtaining $r = xr_{\text{min}}$ which is distributed in a way that the uniform time sampling would give. This is computationally efficient, and can be done several times per each simulated trajectory. We have checked that the resulting distribution of r agrees with the directly measured one.

Fig. 1 shows the resulting distributions as a function of r/\bar{R} , where \bar{R} is the initial radius of the cloud. The actual star radius is also indicated on the plot. The lower curve shows the fraction $n(r)$ of particles that are, in a given moment of time, within the radius r from the center. Points with errors represent the results of the simulation. The straight line is a fit by the power law $n(r) \propto r^{1.5}$. Bearing in mind that $n(r)$ is proportional to the density integrated up to the radius r , we conclude that $\rho(r) \propto r^{-1.5}$, in agreement with the results of Ref. [13].

The upper curve shows the fraction $\nu(r)$ of particles whose orbits have periastra within the radius r . One can see that the fraction of such orbits is larger than $n(r)$. The reason is that, after the adiabatic contraction, a considerable amount of DM particles have very elongated orbits and spend most of their time outside the region of radius r . Indeed, $\nu(r)$ scales differently, $\nu(r) \propto r$. The ratio of the two curves gives the enhancement factor as a function of the radius. At the star radius $r = R_\odot$ this factor is $\nu(R_\odot)/n(R_\odot) = 1.84 \times 10^3$.

A few comments are in order. First, the number of simulated trajectories is sufficient to directly measure $\nu(r)$ and almost sufficient to measure $n(r)$ – the required extrapolation in the latter case is by a factor of a few only. Second, we have checked that the results do not depend on the duration T of the baryon contraction as long as $T \gtrsim 3t_{\text{ff}}$. This means that the adiabatic approximation is a good approximation as long as $T \gtrsim 3t_{\text{ff}}$. Remark that

the natural timescale of the star formation is $T \gg t_{\text{ff}}$ [17]. Finally, we would like to point out that our results are in agreement with the Liouville's theorem which requires the phase space density of DM particles to stay constant during the star formation process. This implies that the density of DM after the contraction cannot be more cuspy than $\rho \propto r^{-1.5}$, which is satisfied in our simulations. The distribution in periastra, on the contrary, has no straightforward limitations from the Liouville's theorem.

To summarize, as a result of the formation of a star, the DM bound to the prestellar core experiences the adiabatic contraction and develops a cuspy profile with the density $\rho \propto r^{-1.5}$. Moreover, the distribution of the DM particles in orbits becomes such that there are much more particles that *ever* come within given radius r than there *are* with r at any given moment. For $r = R_{\odot}$ the enhancement factor is $\sim 2 \times 10^3$. Whether all these DM particles can be finally captured by the star depends on whether there is enough time. As a concrete example, in the next section we work out the implications of this enhancement factor for the case of PBHs as DM candidates.

III. CONSTRAINTS ON PBH

A. Existing constraints

For completeness, we start with the brief summary of the already existing constraints. Depending on the mass of PBHs, different effects result in constraints on their fraction. First, PBHs with masses $m_{\text{BH}} \leq 5 \times 10^{14} \text{ g}$ evaporate through Hawking's radiation in a time shorter than the age of the Universe, making them unviable DM candidate. At higher masses, although PBHs are able to survive until present epoch, they evaporate too efficiently and overproduce the observed γ -ray background unless their mass is larger than (a few) $\times 10^{16} \text{ g}$ [18–20].

For PBHs with masses $m_{\text{BH}} \geq 10^{17} \text{ g}$ the Hawking radiation is negligible. Still, constraints can be imposed by looking at microlensing effects that such PBHs induce when passing in front of a bright source. In this way, the EROS microlensing survey and the MACHO collaboration derived constraints on the fraction of PBHs in the Galactic halo for the range of masses $10^{26} \text{ g} < m_{\text{BH}} < 10^{33} \text{ g}$ [20, 21] that may be improved in the near future [22, 23]. In the same region of masses, the effect of superradiant instabilities of rotating PBHs on the cosmic microwave background has been studied in [24], leading to interesting constraints.

For $m_{\text{BH}} > 10^{33} \text{ g}$, it has been found in [25] that the accretion of gas by PBHs before recombination epoch leads to emission of X-rays that induces changes in the cosmological parameter estimates. Using both data from the three-year Wilkinson Microwave Anisotropy Probe (WMAP3) and the COBE Far Infrared Absolute Spectrophotometer, very stringent constraints have been derived in [25].

In the remaining mass window $10^{17} \text{ g} < m_{\text{BH}} < 10^{26} \text{ g}$, constraints from femtolensing for masses $10^{18} \text{ g} < m_{\text{BH}} < 10^{20} \text{ g}$ have been claimed in Ref. [26]. Finally, considering both the PBH capture at the stage of star formation and during the lifetime, the constraints have been derived in Refs. [12, 13] in the range of masses $10^{16} \text{ g} < m_{\text{BH}} < 10^{24} \text{ g}$ assuming the existence of dense DM cores in globular clusters at the epoch of star formation as would be the case if the latter were of a primordial origin. Note that much more stringent constraints based on the PBH capture by neutron stars have been claimed recently in Ref. [27]. We do not cite these constraints here because we believe that the calculation of Ref. [27] has a problem [28]. The existing constraints are summarized in Fig. 3.

B. Revised constraints on PBH from star formation

The complete information about the DM particle trajectories after the adiabatic contraction allows one to make a more accurate estimate of the number of captured PBHs than it was done in Ref. [13]. Since only the PBHs that can lose energy can be captured, only the trajectories that pass through or in the near vicinity of the star are relevant. To calculate the number of captured PBHs, for each PBH trajectory of this type one has to determine whether there is enough time for the PBH to lose energy and end up in the compact remnant of the star — WD or NS.

Let us sketch the calculation of the capture time. Two stages of the energy loss should be distinguished. At the first stage, the PBH spends part of the time outside the progenitor star. Such orbits can be approximately considered as radial, except a small number of cases when the apastron is of order R_* . In this approximation, the capture time has been estimated in [12] to be of order

$$t_{\text{capt}} \simeq 2\tau \sqrt{\xi_0} \sim 2 \times 10^8 \text{ yrs} \left(\frac{10^{22} \text{ g}}{m_{\text{BH}}} \right), \quad (3)$$

where

$$\tau = \frac{\pi R_*^{5/2} v^2}{4Gm_{\text{BH}} \sqrt{GM} \ln \Lambda},$$

with $\xi_0 = r_{\text{max}}/R_*$, v the escape velocity of the star, $\ln \Lambda$ the Coulomb logarithm [29] that takes a value close to $\ln \Lambda \simeq 30$ for a main-sequence star, and R_* and M the radius and the mass of the star, respectively. For the numerical value in eq. (3) we have taken $r_{\text{max}}/\bar{R} \simeq 0.1$ corresponding to a value of $\xi_0 \simeq 4.4 \times 10^4$. However, when computing the constraints presented below we have used the values of r_{max} corresponding to simulated trajectories, which is the main difference with the estimates of Ref. [13]. In this way we have determined, for each PBH mass, the fraction of simulated PBH orbits that would be captured by the star during its lifetime.

While deriving the constraints, we have also taken into account the PBH orbits that do not cross the star, but come close enough to lose energy through tidal interactions [30]. However, the amount of PBHs captured in this way turned out to be negligible.

The second stage starts when PBH is fully inside the star. It then continues to lose energy through the dynamical friction [31] and gradually sinks towards the star center until the moment when the star turns into a compact remnant. If the radius to which the PBH has been able to sink to during the lifetime of the star is smaller than the radius of the compact remnant, the latter inherits a PBH. The efficiency of the dynamical friction grows with the PBH mass. At large masses all the PBH captured by a star have time to sink to within the radius of the future remnant in a lifetime of the star. At small masses only a fraction of captured PBH can make it. At the second stage there is no difference with the calculations of Ref. [13]. Combining the two stages gives the fraction of the PBHs that ends up inside the compact remnant.

The final step in deriving the constraints consists in relating the number of simulated trajectories with the mean density of DM in a given environment. This can be done as described in Ref. [13] by calculating the fraction of the DM particles which are gravitationally bound to the prestellar core before the adiabatic contraction. An important point to keep in mind is that this fraction is proportional to the total DM density and inversely proportional to the cube of the DM velocity dispersion. Making use of this scaling, the results for one particular DM density and velocity dispersion can be rescaled to other values of these parameters.

To summarize, the difference between the present calculation and Ref. [13] is that there it was assumed that only PBHs that are within the star at a given moment after the end of the adiabatic contraction are captured by the star and may end up inside the compact remnant, provided they sink sufficiently close to the center by the time the remnant is formed. On the contrary, in the present calculation all PBH trajectories that ever pass through the star are taken into account. Whether there is sufficient time for a PBH to be captured by the star is calculated individually for each trajectory. The distribution of PBH over parameters of the orbits is taken directly from the simulation.

The resulting constraints are shown in Fig. 2. To obtain these constraints we have considered stars with masses $M_\odot \leq M \leq 7M_\odot$, the progenitors of WDs, and stars with $8M_\odot \leq M \leq 15M_\odot$ which become NSs. WDs lead to better constraints for low PBHs masses, while NSs are more competitive at high masses. The transition between the two regimes is around $m_{\text{BH}} \sim 10^{20}$ g. For comparison, the constraints of Ref. [13] are also presented in Fig. 2. Both constraints are derived assuming the velocity dispersion of $\bar{v} = 7$ km/s. Such velocities are characteristic of globular clusters and dwarf spheroidal galaxies. The values for other densities and velocity dispersions can be obtained by a simple rescaling as de-

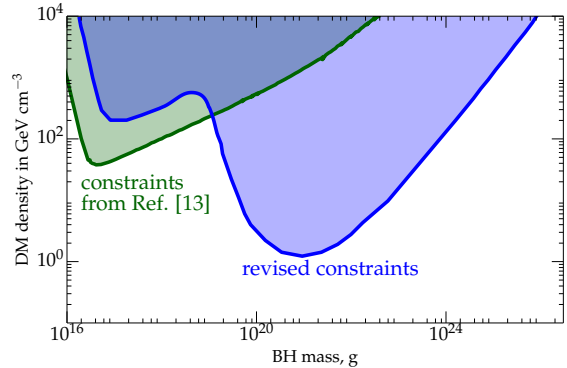


FIG. 2: Constraints on the abundance of PBHs assuming the DM velocity dispersion of 7 km/s. The constraints derived in Ref. [13] are in green, while the revised ones are in blue.

scribed above.

At large PBH masses, the revised constraints are substantially more stringent than those of Ref. [13]. In this mass range the energy loss mechanism is so efficient that all the gravitationally bound PBH that ever cross the star have time to be captured and transferred to a compact remnant. As pointed out in Sect. II, the number of such trajectories turned out to be much larger than it was assumed in Ref. [13]. In this range of masses the gain in the total captured mass (and therefore, the improvement in the constraints) is the ratio between the two curves of Fig. 1 calculated at $r = R_* \sim R_\odot$, which is close to 1.8×10^3 . For stellar masses $M_* > 8M_\odot$, this number is reduced by a factor two.

At small PBH masses, the revised constraints are, on the contrary, somewhat worse than the estimate of Ref. [13]. The reason for this is that some of the PBH that are inside the star by the end of the adiabatic contraction, are in fact on elongated orbits and spend most of the time outside the star. When the energy losses are not efficient, these PBH do not have enough time to lose their energy and get captured by the star. Such orbits were, but should not have been, included in the estimates in Ref. [13], hence the difference.

Clearly, most stringent constraints come from observations of compact stars in regions with a high DM density and a low DM velocity dispersion. As a benchmark, we consider the values $\rho_{\text{DM}} \sim 10^4$ GeVcm $^{-3}$ and $\bar{v} = 7$ km s $^{-1}$. The constraints that would result in this case are shown in Fig. 3 together with the other existing constraints. The corresponding conditions may be present in the cores of metal-poor globular clusters at the epoch of star formation, if they are proved to be of a primordial origin [32] (see detailed discussions in [12, 13]). Another place where similar conditions, albeit with somewhat lower densities, could exist are dwarf spheroidal galaxies that are considered to be DM dominated [33, 34] and have very low velocity dispersions [33]. However, at present compact objects such as NS or WD have not been

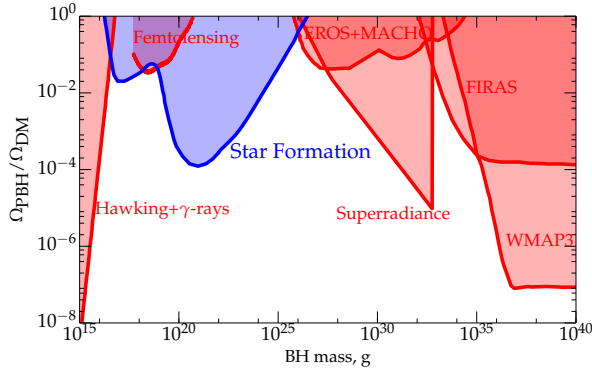


FIG. 3: Constraints on the fraction of PBHs as DM. Shaded regions are excluded. The blue shaded region corresponds to the revised constraints derived in this paper assuming the DM density of 10^4 GeV/cm^3 and the velocity dispersion of 7 km/s . The red shaded regions represent the existing constraints coming from various observations as explained in Sect. III A.

observed in dwarf spheroidal galaxies. Nonetheless, surveys for pulsars, fast radio transients and X-ray binaries have already revealed some glimpses of NSs existence in dSph galaxies [35, 36], even though a clear observation is still lacking.

IV. CONCLUSIONS

In this paper we have considered the adiabatic contraction of DM during the formation of a star. By simulating the behavior of ~ 30 million particles, we reconstructed the phase space distribution of the DM at the end of the star formation. In particular, the number of particles $n(r)$ within a given radius r was found to be proportional to $r^{1.5}$, which corresponds to the DM density profile $\rho(r) \propto r^{-1.5}$, in agreement with previous calculations and the Liouville theorem.

At the same time, we have found that the adiabatic contraction creates a rather special distribution of particle orbits. Namely, if one considers the particles that contribute to $n(r)$ for a small r , a substantial ($O(1)$) fraction of them have very elongated orbits with periastra smaller than r . In fact, the number of particles $\nu(r)$ that have periastra smaller than r scales as $\nu(r) \propto r$. Such particles spend only a small fraction of time close to the

center, so their individual contributions to the density at small r are suppressed. However, they are numerous enough to contribute non-negligibly to the density. At $r = R_\odot$, there are about 1.8×10^3 more particles that have periastra smaller than r than there are particles within r .

This has implications for the DM capture by stars after their formation. A large number of particles that constitute the DM cusp around the newly-formed star have orbits that cross the star, which potentially leads to their capture. This factor has not been taken into account in the previous estimates.

As an application, we have considered the capture of PBH by stars, which leads to the constraints on the PBH abundance. We have recalculated the constraints of Ref. [13] computing capture times individually for each trajectory, and taking trajectories directly from the simulation of the adiabatic contraction. In the range of PBH masses $10^{20} \text{ g} \lesssim m_{\text{BH}} \lesssim 10^{26} \text{ g}$, the constraints are improved by about 3 orders of magnitude due to the enhancement factor discussed above. The resulting constraints are shown in Fig. 2.

The most stringent constraints are obtained from observations of compact stars in the regions with high DM density and small velocity dispersion. The example corresponding to the density $\rho = 10^4 \text{ GeV cm}^{-3}$ and a low velocity dispersion $\bar{v} = 7 \text{ km s}^{-1}$ is shown in Fig. 3. Such conditions could have been present at the cores of metal-poor globular clusters at the epoch of star formation if they are of a primordial origin [32], or with a somewhat smaller DM density in dwarf spheroidal galaxies [33, 34, 37]. However, clear observations of compact objects in dwarf spheroidals are still lacking.

Acknowledgments

The authors are indebted to Michel Tytgat and Malcolm Fairbairn for valuable discussions and comments. M.P. acknowledges the hospitality of the Service de Physique Théorique of ULB where this work was initiated. The work of F.C. and P.T. is supported in part by the IISN and the Belgian Science Policy Belgian Science Policy under IUAP VII/37. The work of M.P. is supported by RFBR Grants No. 13-02-01311a, No. 13-02-01293a, by the Grant of the President of Russian Federation MK-2138.2013.2 and by the Dynasty Foundation.

-
- [1] Planck Collaboration, P. A. R. Ade, N. Aghanim, C. Armitage-Caplan, M. Arnaud, M. Ashdown, F. Atrio-Barandela, J. Aumont, C. Baccigalupi, A. J. Banday, et al., ArXiv e-prints (2013), 1303.5076.
 - [2] S. Nussinov, L.-T. Wang, and I. Yavin, JCAP **8**, 037 (2009), 0905.1333.
 - [3] I. Lopes and J. Silk, Astrophys.J. **757**, 130 (2012), 1209.3631.
 - [4] J. Casanellas and I. Lopes, Astrophys.J. **L21** (2013), 1212.2985.
 - [5] J. Casanellas and I. Lopes (2013), 1307.6519.
 - [6] M. T. Frandsen and S. Sarkar, Phys.Rev.Lett. **105**, 011301 (2010), 1003.4505.
 - [7] C. Horowitz (2012), 1205.3541.

- [8] C. Kouvaris and P. Tinyakov, Phys.Rev. **D83**, 083512 (2011), 1012.2039.
- [9] C. Kouvaris and P. Tinyakov, Phys.Rev. **D82**, 063531 (2010), 1004.0586.
- [10] C. Kouvaris and P. Tinyakov, Phys.Rev.Lett. **107**, 091301 (2011), 1104.0382.
- [11] C. Kouvaris and P. Tinyakov (2013), 1312.3764.
- [12] F. Capela, M. Pshirkov, and P. Tinyakov, Phys.Rev. **D87**, 123524 (2013), 1301.4984.
- [13] F. Capela, M. Pshirkov, and P. Tinyakov, Phys.Rev. **D87**, 023507 (2013), 1209.6021.
- [14] G. Jungman and M. Kamionkowski, Phys. Rev. D **51**, 328 (1995), hep-ph/9407351.
- [15] T. C. Mouschovias and S. A. Morton, Astrophys. J. **371**, 296 (1991).
- [16] F. H. Shu, F. C. Adams, and S. Lizano, ARA&A **25**, 23 (1987).
- [17] T. Wong, Astrophys. J. **705**, 650 (2009), 0909.2243.
- [18] B. Carr, K. Kohri, Y. Sendouda, and J. Yokoyama, Phys.Rev. **D81**, 104019 (2010), astro-ph/0912.5297.
- [19] P. Sreekumar et al. (EGRET Collaboration), Astrophys.J. **494**, 523 (1998), astro-ph/9709257.
- [20] C. Alcock, R. A. Allsman, D. Alves, R. Ansari, E. Aubourg, T. S. Axelrod, P. Bareyre, J.-P. Beaulieu, A. C. Becker, D. P. Bennett, et al., Astrophys. J. Lett. **499**, L9 (1998), astro-ph/9803082.
- [21] P. Tisserand et al. (EROS-2 Collaboration), Astron.Astrophys. **469**, 387 (2007), astro-ph/0607207.
- [22] A. M. Cieplak and K. Griest, Astrophys. J. **767**, 145 (2013), 1210.7729.
- [23] K. Griest, A. M. Cieplak, and M. J. Lehner, ArXiv e-prints (2013), 1307.5798.
- [24] P. Pani and A. Loeb, Phys. Rev. D **88**, 041301 (2013), 1307.5176.
- [25] M. Ricotti, J. P. Ostriker, and K. J. Mack (2007), 0709.0524.
- [26] A. Barnacka, J.-F. Glicenstein, and R. Moderski, Phys. Rev. D **86**, 043001 (2012), 1204.2056.
- [27] P. Pani and A. Loeb, ArXiv e-prints (2014), 1401.3025.
- [28] F. Capela, M. Pshirkov, and P. Tinyakov, ArXiv e-prints (2014), 1402.4671.
- [29] J. Binney and S. Tremaine, *Galactic dynamics* (1987).
- [30] W. H. Press and S. A. Teukolsky, Astrophys. J. **213**, 183 (1977).
- [31] S. Chandrasekhar, Reviews of Modern Physics **21**, 383 (1949).
- [32] G. Bertone and M. Fairbairn, Phys.Rev. **D77**, 043515 (2008), 0709.1485.
- [33] L. E. Strigari, S. M. Koushiappas, J. S. Bullock, M. Kaplinghat, J. D. Simon, M. Geha, and B. Willman, Astrophys. J. **678**, 614 (2008), 0709.1510.
- [34] L. E. Strigari, S. M. Koushiappas, J. S. Bullock, and M. Kaplinghat, Phys. Rev. D **75**, 083526 (2007), astro-ph/0611925.
- [35] E. Rubio-Herrera and T. Maccarone, in *IAU Symposium* (2013), vol. 291 of *IAU Symposium*, pp. 111–114.
- [36] T. J. Maccarone, A. Kundu, S. E. Zepf, A. L. Piro, and L. Bildsten, Mon. Not. R. Astron. Soc. **364**, L61 (2005), arXiv:astro-ph/0509427.
- [37] P. Salucci, M. I. Wilkinson, M. G. Walker, G. F. Gilmore, E. K. Grebel, A. Koch, C. Frigerio Martins, and R. F. G. Wyse, Mon. Not. R. Astron. Soc. **420**, 2034 (2012), 1111.1165.